Chapter 5

Simulation Results

As it was said in the previous chapter, scaled human values were taken to the parameters of stiffness and damping. It was one of the goals of this job to make a sensitivity analysis of the influence of the main parameters in the behavior of the model. According to this analysis, a adjustment process were carried out to fit the frequency response of the model with the available experimental results.

5.1 Sensitivity Analysis

One of the goal of this work was to get a first eigenfrequency and first eigenmode in agreement with literature data. According to the experimental results[9] it is possible to see that, while for high eigenfrequencies there are significant rocking motions in the stapes, for low frequencies, these movements are, practically, not significant. That means a piston-like motion of the stapes. Therefore, the first eigenmode consists, mainly, in a rocking motion of the MIC around the axis which goes from the point $KH5$ to the point $KA1$ (see fig.4.8) and a piston-like motion of the stapes. Thus, due to the high number of model parameters, in the sensitivity analysis they were only taken in count those parameters which have influence in this kind of motion. These parameters were the rotational springs around the x direction of the ligamentum mallei anterious, the ligamentun incudus posterius and the incudo-stapedial joint, and the translational springs in the y direction of the incudo-stapedial joint, the annular ring and the tympanic membrane. Besides, due to the existence of certain motion in the y direction of the ligamentum mallei anterious and the ligamentun incudus posterius,

their stiffness in this direction were included in the analysis.

The analysis was carried out from two points of view. The first one was about the influence of the model parameters in the static response of the system. The second one was about the influence of the model parameters in the three first eigenfrequencies. The system response was defined through its transfer function as it is shown in the equation 5.1.

$$f(\omega) = \frac{Y_{stapes}}{Y_{umbo}} \tag{5.1}$$

where Y_{stapes} is motion of the stapes in the y direction and Y_{umbo} is the umbo motion in the y direction as well. However, although this is proper definition from a mechanical point of view, it is usual to find out in the literature another definition of the transfer function more in agreement with a acoustical point of view where the y-motion of the stapes is divided by the pressure on the tympanic membrane (see eq. 5.2). It was used here this definition since the experimental data available were in this way.

$$f(\omega) = \frac{Y_{stapes}}{P} \tag{5.2}$$

5.1.1 Sensitivity Analysis of the Model Parameters on the Static Response

At the range of low frequencies where hinge-like rotation is a dominant motion of the MIC, the pressure gain through the middle ear is presumed to be provided by the area ratio between the tympanic membrane and the footplate of the stapes and the lever ratio in the hinge-like motion of the MIC [9]. The lever ratio was already measured in this model (see chapter 4) and its value was 2.045. The footplate area was measured as well providing a value of 0.9 mm^2, which is in range with experimental data [9]. Thus, in the following figures the frequency response at a low frequency (10 Hz) is shown.

5.1.2 Sensitivity Analysis of the Model Parameters on the Three First Eigenfrequencies

In the following figures the influence of the model parameters in the three first eigenfrequencies are shown.

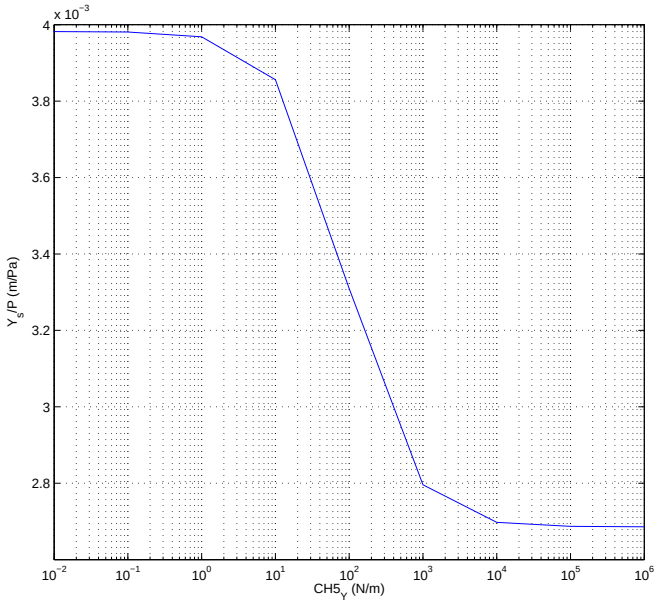

Figure 5.1: Evolution of the static response over the parameter *CH5Y*.

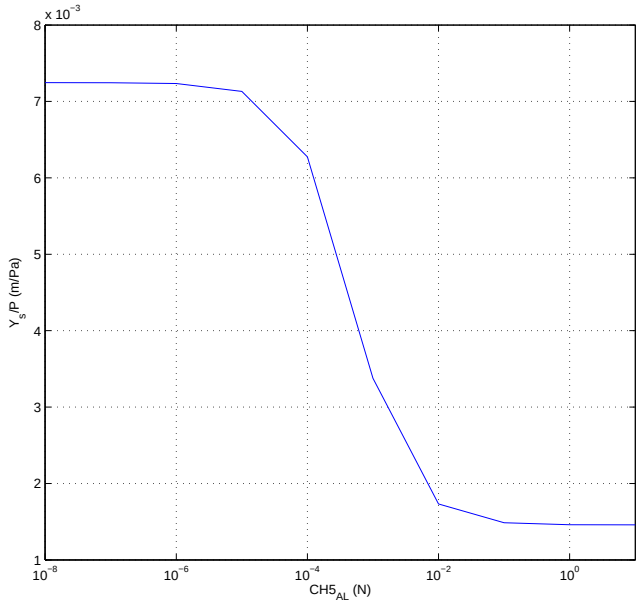

Figure 5.2: Evolution of the static response over the parameter *CH5AL*.

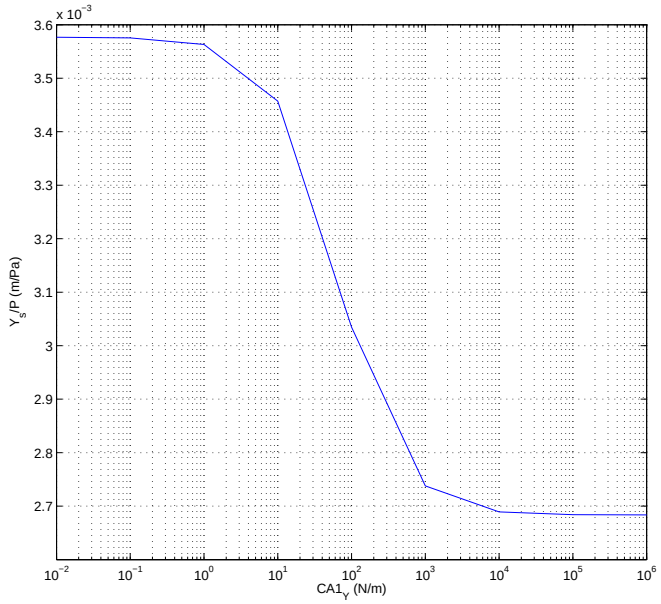

Figure 5.3: Evolution of the static response over the parameter *CA1Y*.

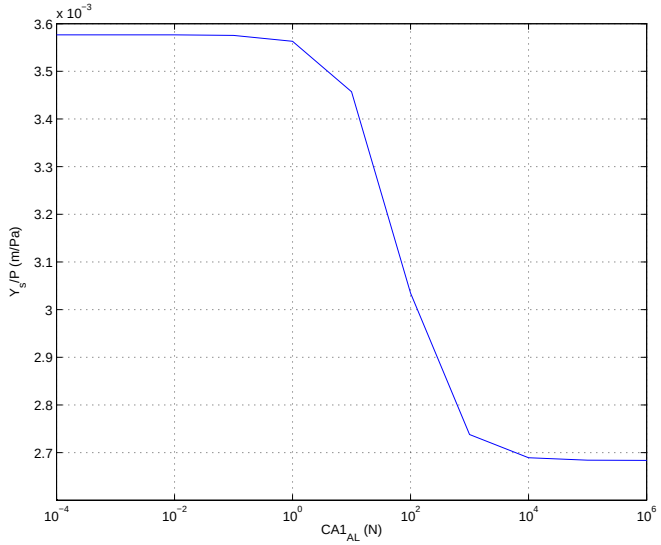

Figure 5.4: Evolution of the static response over the parameter *CA1AL*.

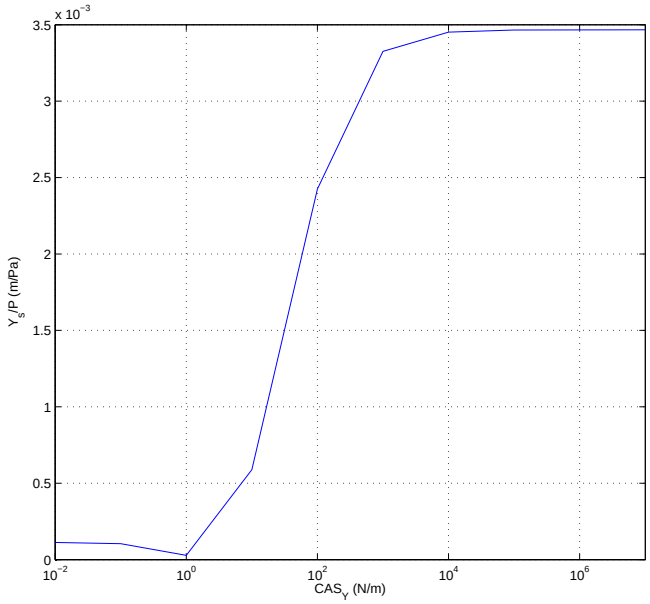

Figure 5.5: Evolution of the static response over the parameter *CASY*.

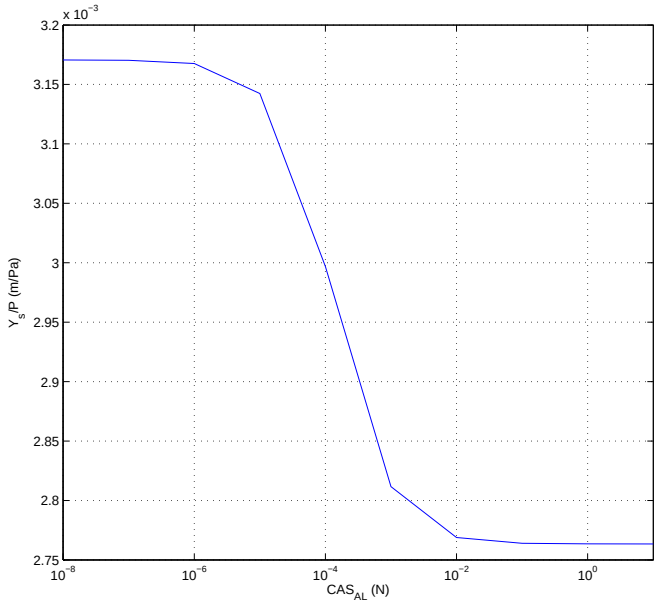

Figure 5.6: Evolution of the static response over the parameter *CASAL*.

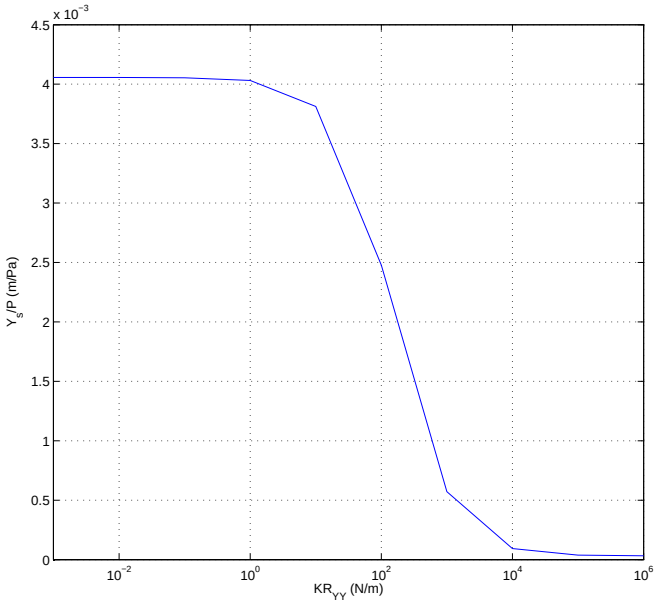

Figure 5.7: Evolution of the static response over the parameter *KRYY*.

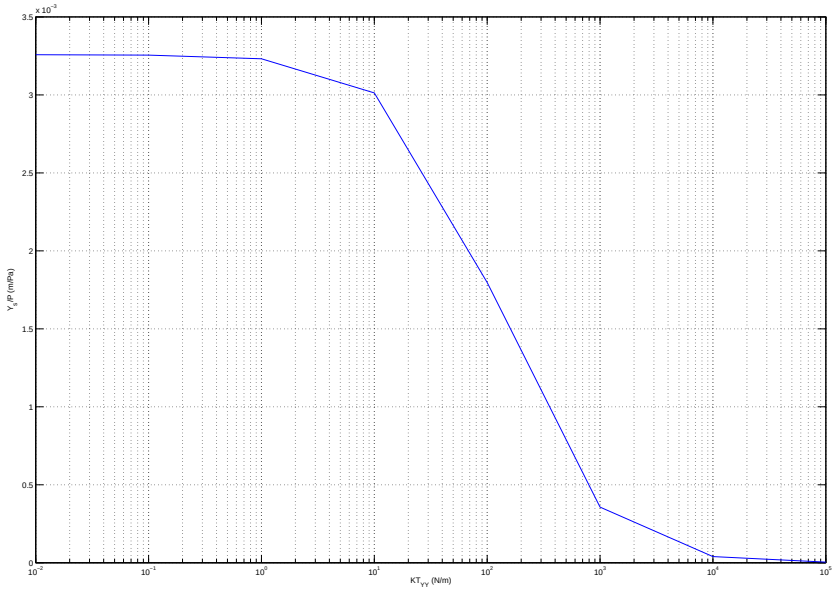

Figure 5.8: Evolution of the static response over the parameter *KTYY*.

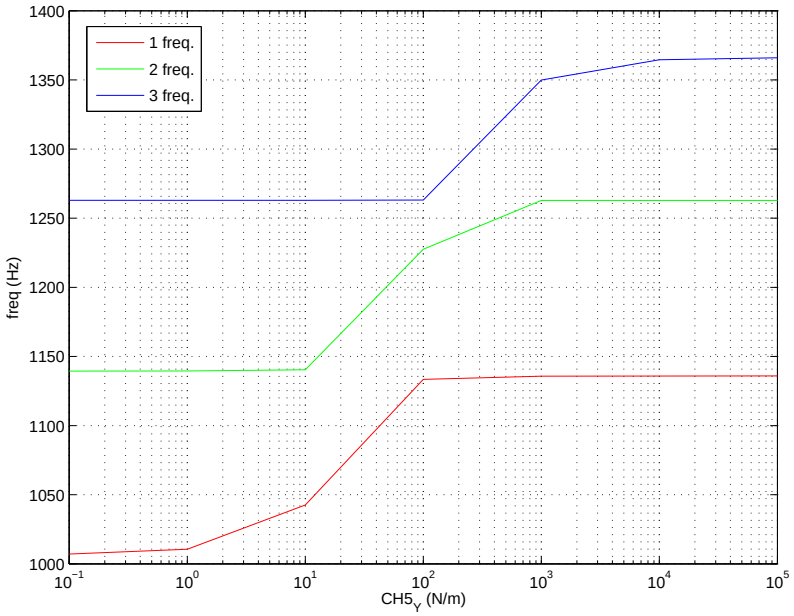

Figure 5.9: Evolution of the three first eigenfrequencies over the parameter *CH5Y*.

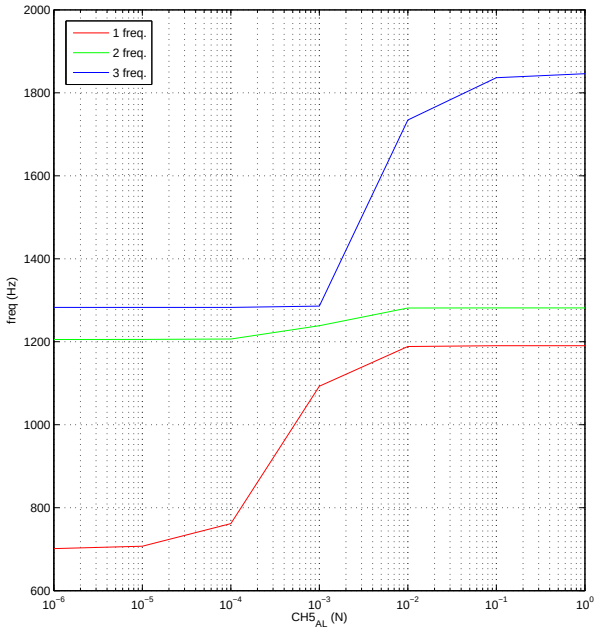

Figure 5.10: Evolution of the three first eigenfrequencies over the parameter *CH5AL*.

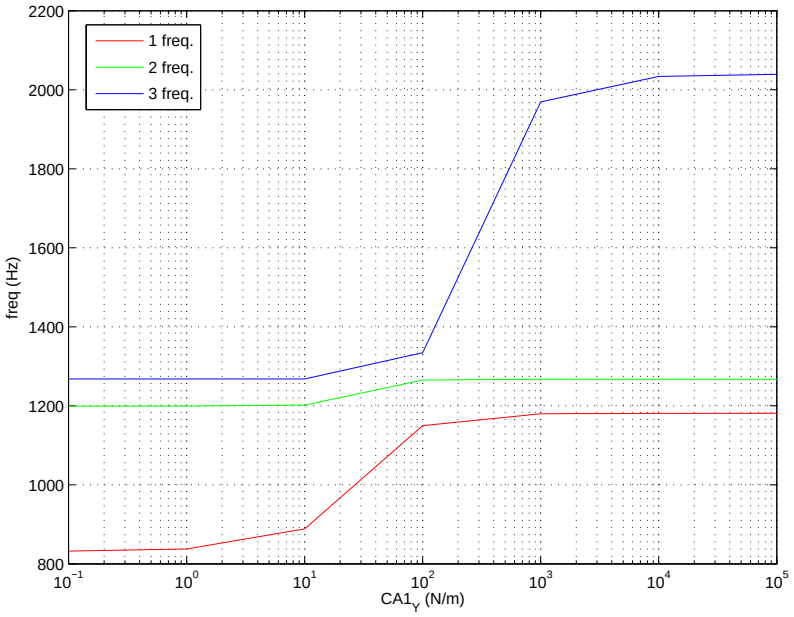

Figure 5.11: Evolution of the three first eigenfrequencies over the parameter *CA1Y*.

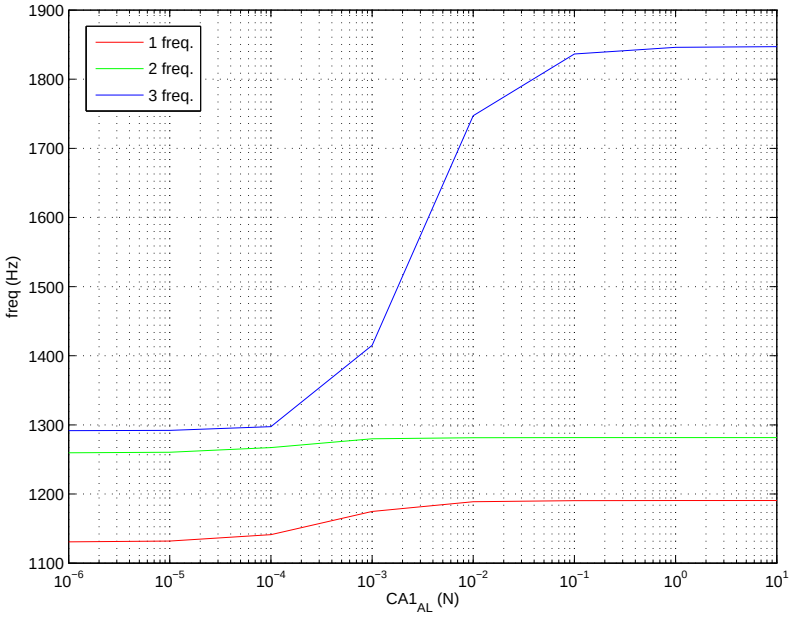

Figure 5.12: Evolution of the three first eigenfrequencies over the parameter *CA1AL*.

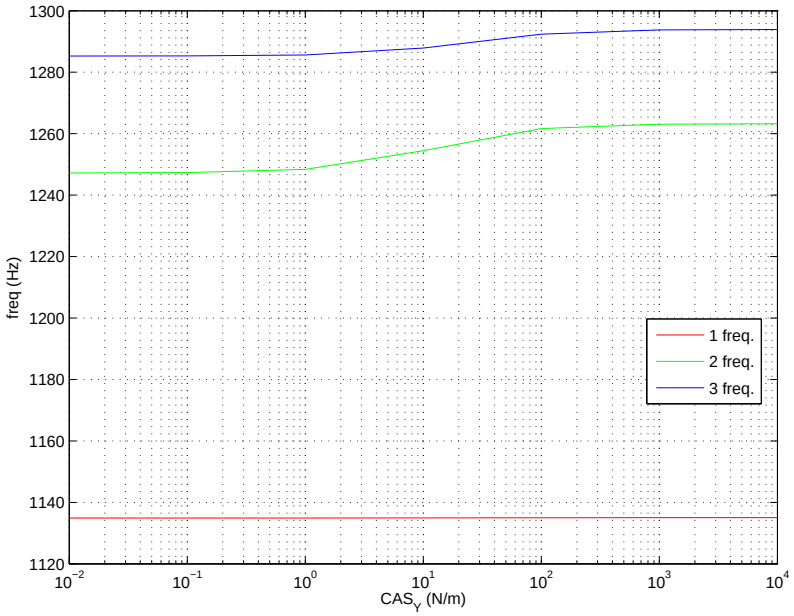

Figure 5.13: Evolution of the three first eigenfrequencies over the parameter *CASY*.

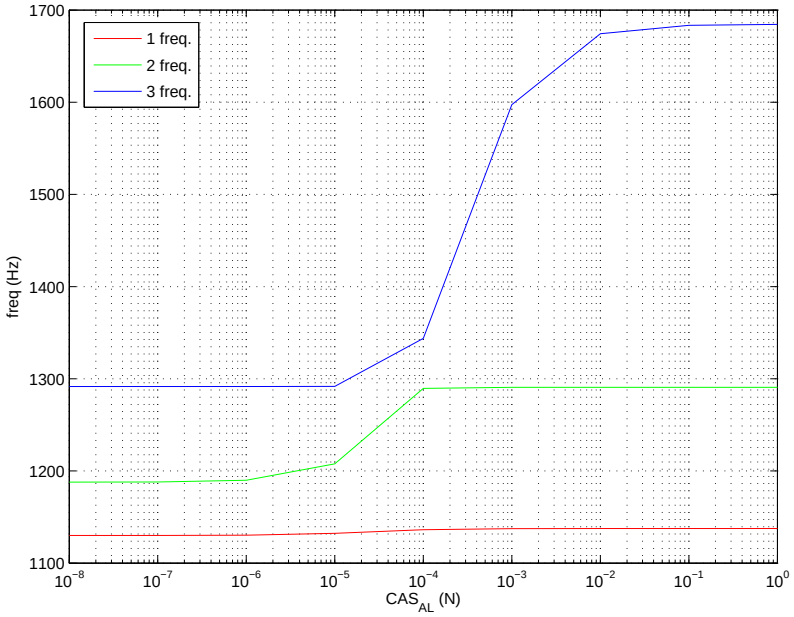

Figure 5.14: Evolution of the three first eigenfrequencies over the parameter *CASAL*.

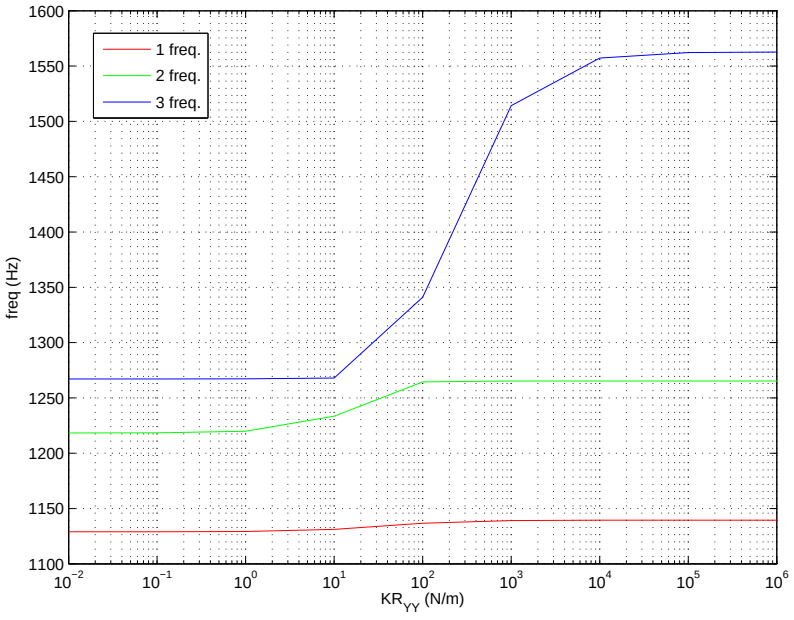

Figure 5.15: Evolution of the three first eigenfrequencies over the parameter *KRYY*.

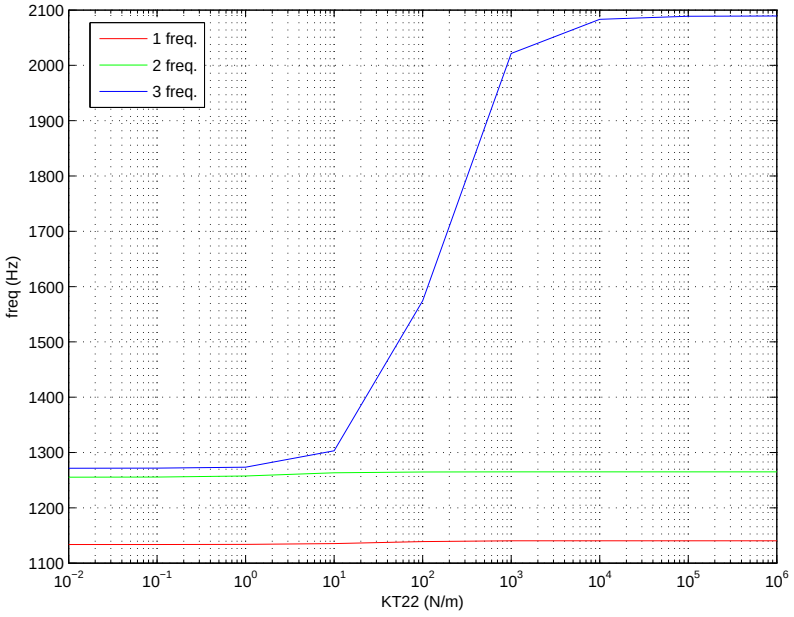

Figure 5.16: Evolution of the three first eigenfrequencies over the parameter *KTYY*.

5.2 Adjustment of the Model Parameters to Measurement Data

According to the sensitivity analysis results, the model parameters were adjusted in order to fit the response of the model with the experimental data. Thus, in table 5.1 the previous and final values of the parameters are shown as well as in the figure 5.17 it is shown what the influence of this changes in the transfer function magnitude was. With these new values the transfer function were calculated as well as the frequency response of the rocking motions.

Parameter	Initial value	Final value
CH5Y	216.6	516.6
CH5AL	$12.8 \cdot 10^{-4}$	$42.8 \cdot 10^{-4}$
CA1Y	83.3	433
CA1AL	$3.83 \cdot 10^{-5}$	$9.83 \cdot 10^{-5}$
CASY	333.3	33330
CASAL	$4.16 \cdot 10^{-5}$	$4.16 \cdot 10^{-5}$
KRYY	50	50
KTYY	7.35	7.35

Table 5.1: Initial and final values of the parameters taken in count. All the values are in the I.S.

5.2.1 Transfer Function Compared to Measurements.

In the following figures (figs. 5.18 and 5.19) the magnitude and phase of the transfer function are shown and compared with measurement data from Sim [9] and Daholff[1].

In order to analyze the results, it was possible to see that the model was in agreement with experimental results around the first eigengrequency (around 2000 Hz). This value was also in agreement with literature data ([6]) It was possible to see that, while transfer function phase of the model fitted with Dalhoff's results, there was a big difference with Sim's results. This difference was due to in the process of measure was introduced a fictitious eigenfrequency. This was the reason of the difference (around 180 degrees) between the two curves in the low frequencies range.

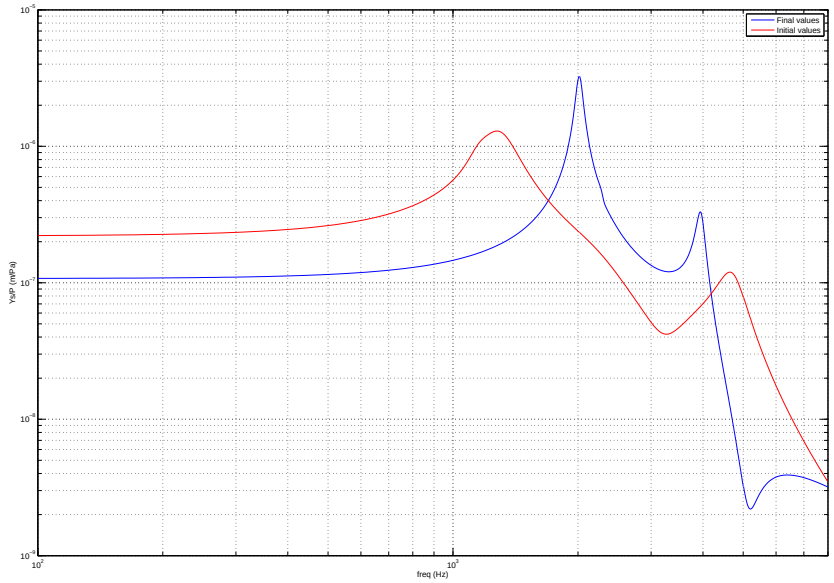

Figure 5.17: Transfer function magnitude with initial and final values of the parameters.

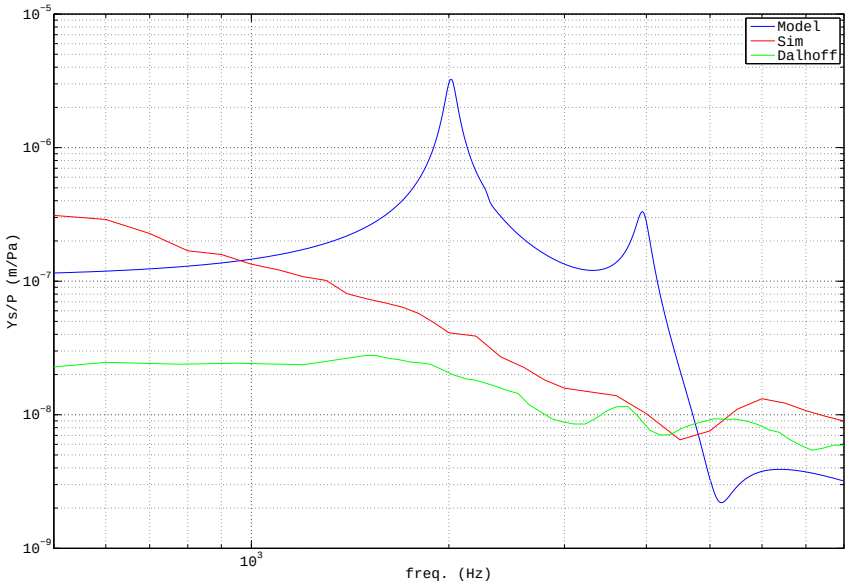

Figure 5.18: Transfer function magnitude. In blue, model transfer function magnitude. In red, data transfer function magnitude from Sim. In green, data transfer function magnitude from Dalhoff.

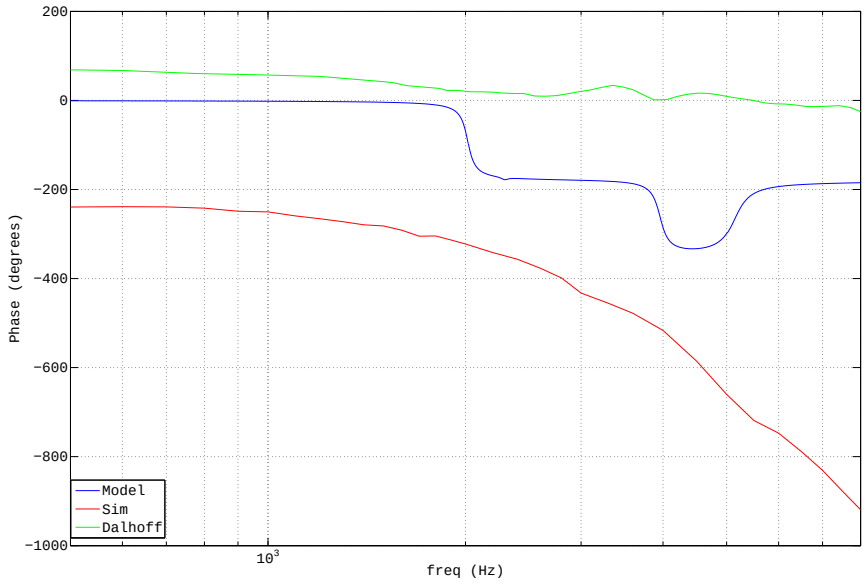

Figure 5.19: Transfer function phase. In blue, model transfer function phase. In red, data transfer function phase from Sim. In green, data transfer function phase from Dalhoff.

5.2.2 Rocking Motions Compared with Measurements

In the figures 5.20, 5.21, 5.22 and 5.23 the frequency response of the rocking motions (magnitude and phase) are shown and compared with Sim results[9].

It is possible to see that the magnitude of the frequencie response of the rocking motions is not in agreement with the experimental results although the value of the first eigenfrequency is in range. In the case of the phase diagram, there was a diference in the low frequencies range due to the experimental situation mentioned above. However, the behaviors of both model and experimental results were very similar.

5.3 Eingenfrequencies and Eingenmodes

In order to get as much information as possible of the model the first eigenfrequencies and eigenmodes were calculated. Thus, the table 5.2 shows the nine first eigenfrequencies of the system.

In the following figures the nine first eigenmodes are shown with an especial atention to

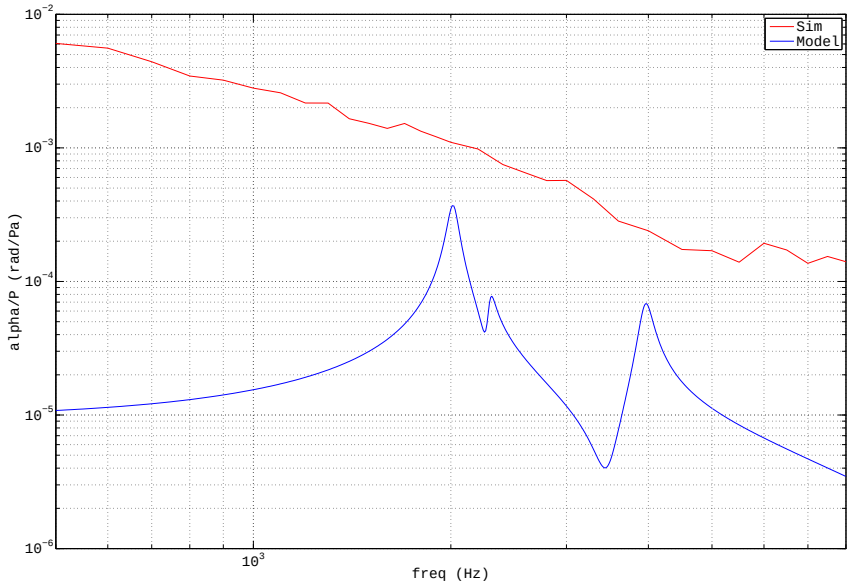

Figure 5.20: α frequency response magnitude. In blue, α frequency response magnitude. In red, α frequency response magnitude from Sim.

Eigenfrequencies	
Number	Value (Hz)
1	2009
2	2285
3	3934
4	8712
5	10128
6	18794
7	25137
8	44710
9	77221

Table 5.2: Nine first eigenfrequencies of the system.

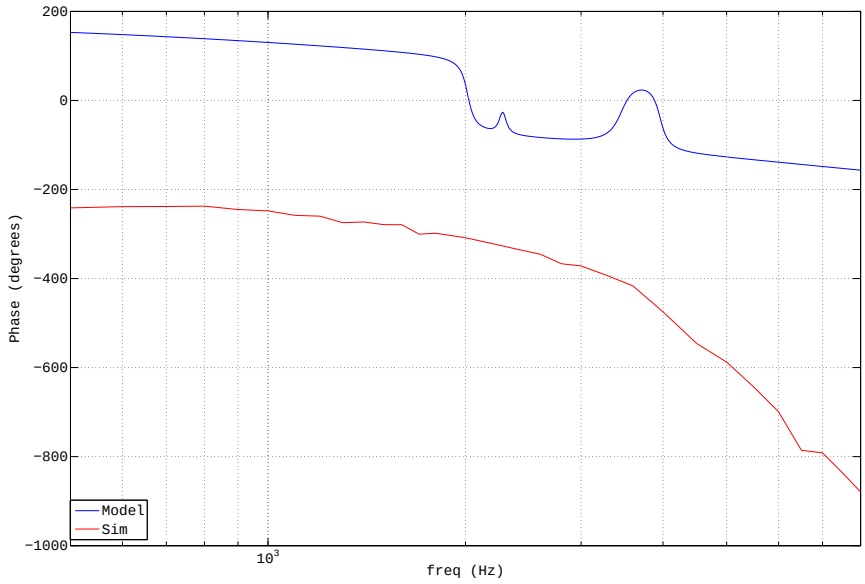

Figure 5.21: α frequency response phase. In blue, α frequency response phase. In red, α frequency response phase from Sim.

the first eigenmode due to the parameters were adjusted in order to get this motion.

It is possible to see that the first eigenmode is in agreement with the expected results: the eigenmode is, mainly, a piston-like motion of the stapes and a hinge-like motion of the MIC. There is a translation in the y direction as well.

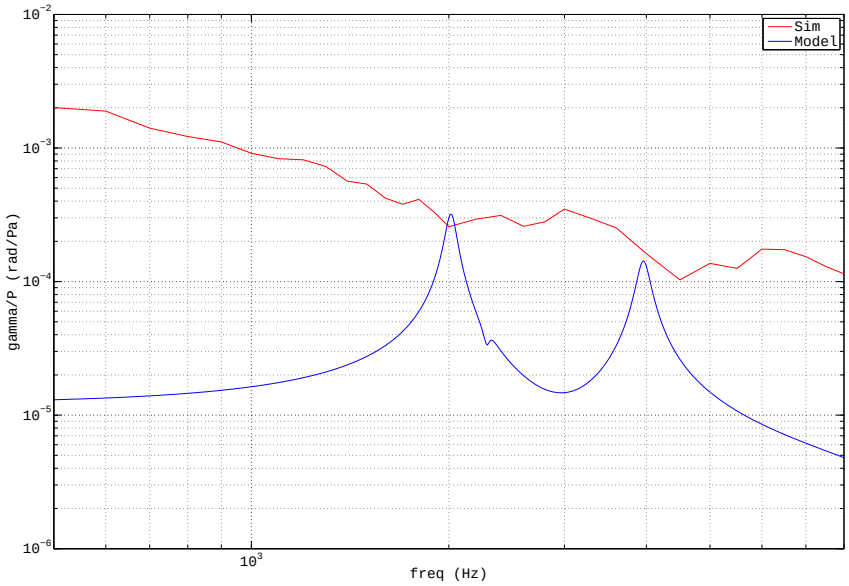

Figure 5.22: γ frequency response magnitude. In blue, α frequency response magnitude. In red, γ frequency response magnitude from Sim.

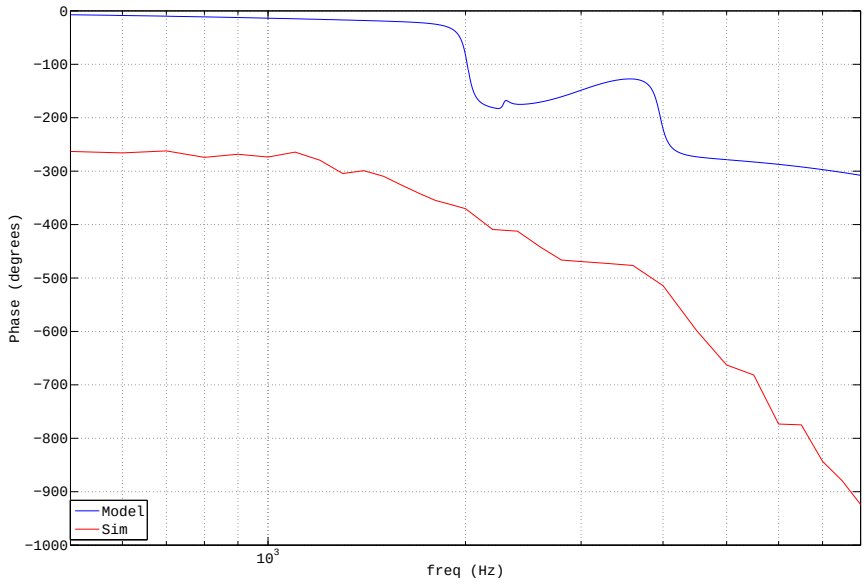

Figure 5.23: γ frequency response phase. In blue, γ frequency response phase. In red, γ frequency response phase from Sim.

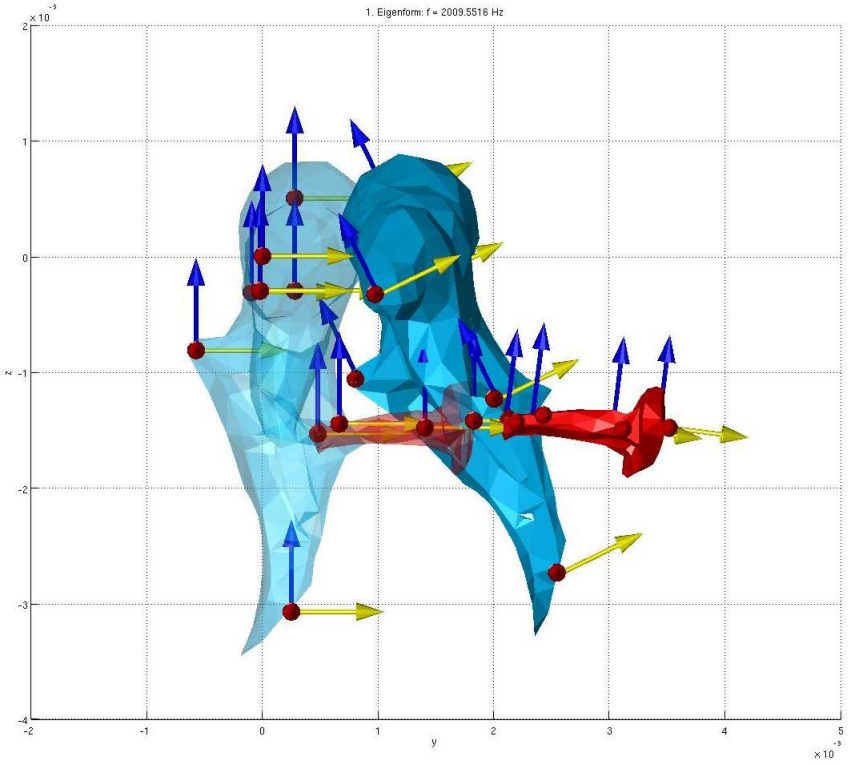

Figure 5.24: View of the first eigenmode in the y-z plane.

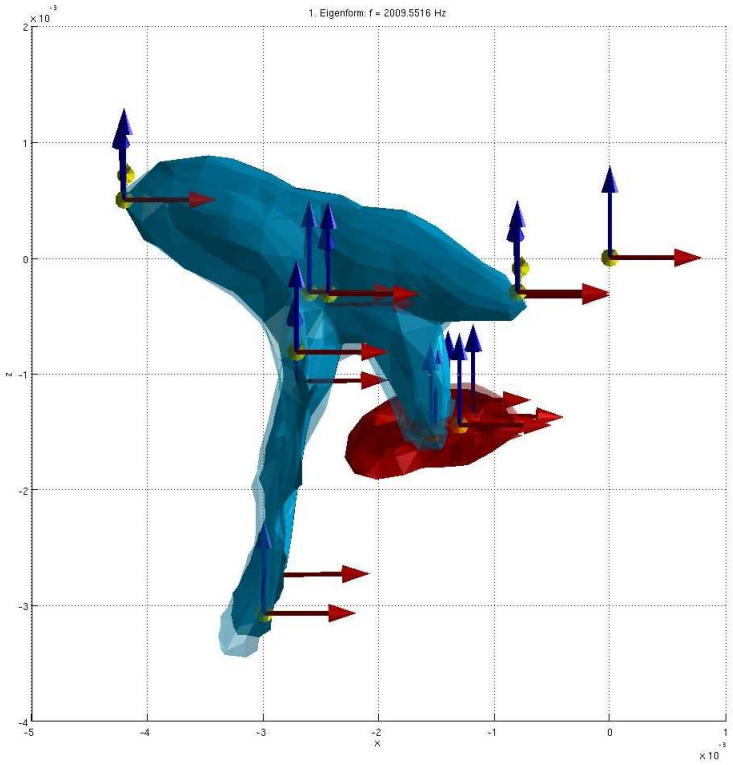

Figure 5.25: View of the first eigenmode in the x-z plane.

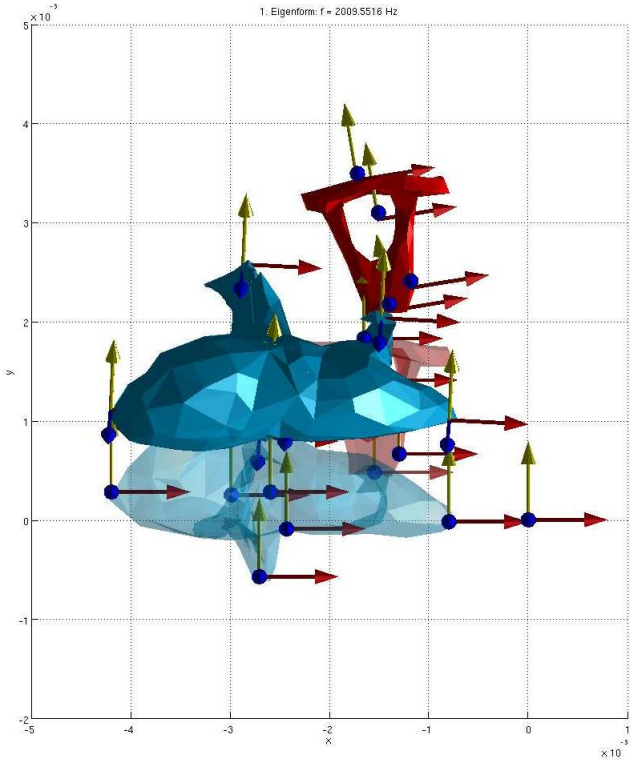

Figure 5.26: View of the first eigenmode in the x-y plane.

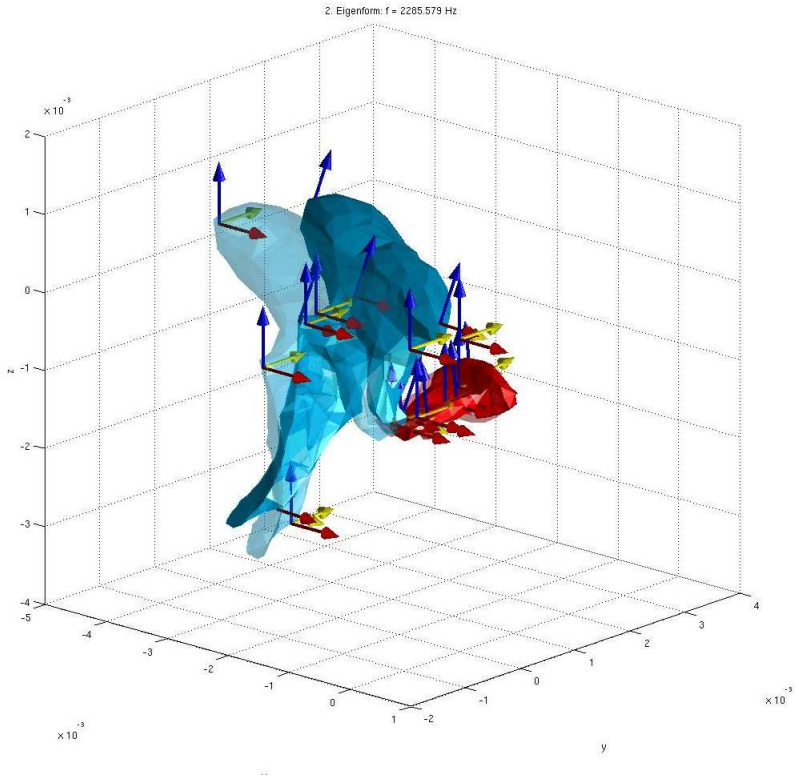

Figure 5.27: View of the second eigenmode.

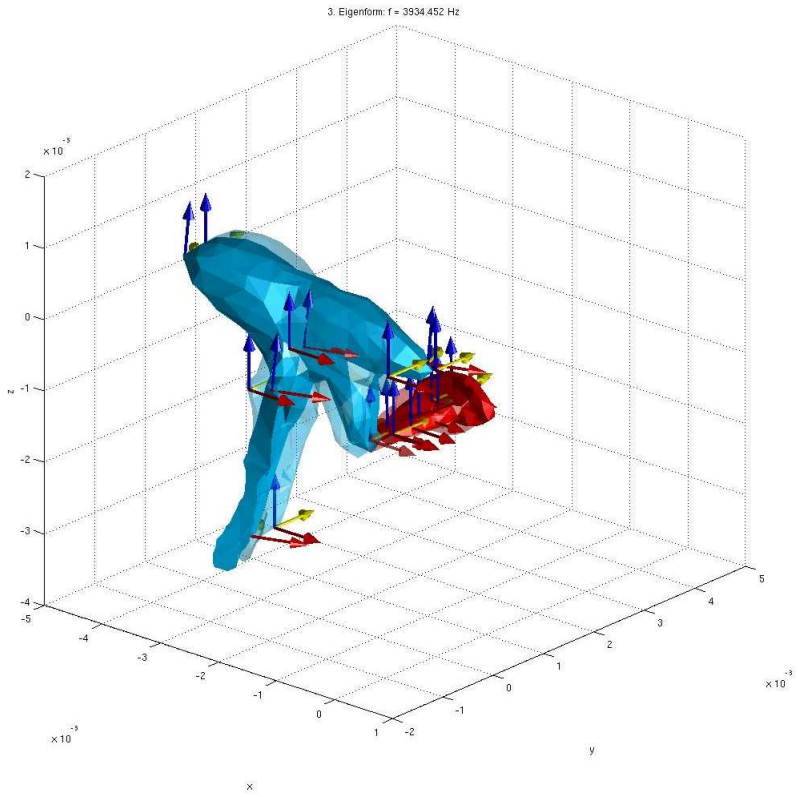

Figure 5.28: View of the third eigenmode.

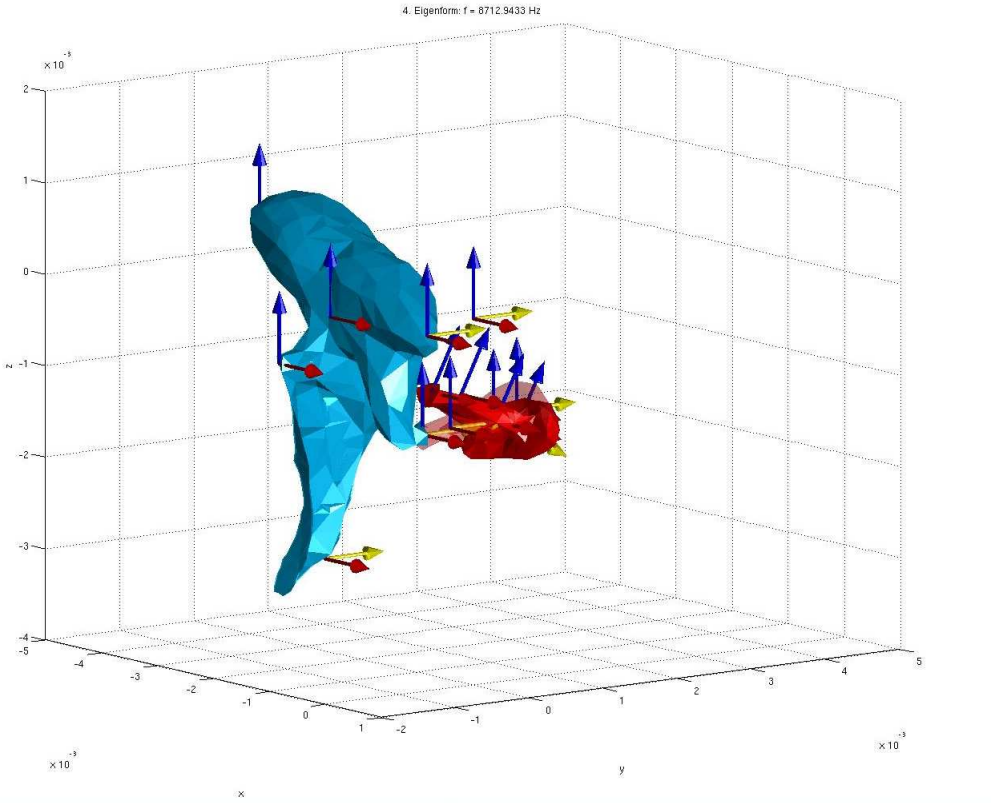

Figure 5.29: View of the fourth eigenmode.

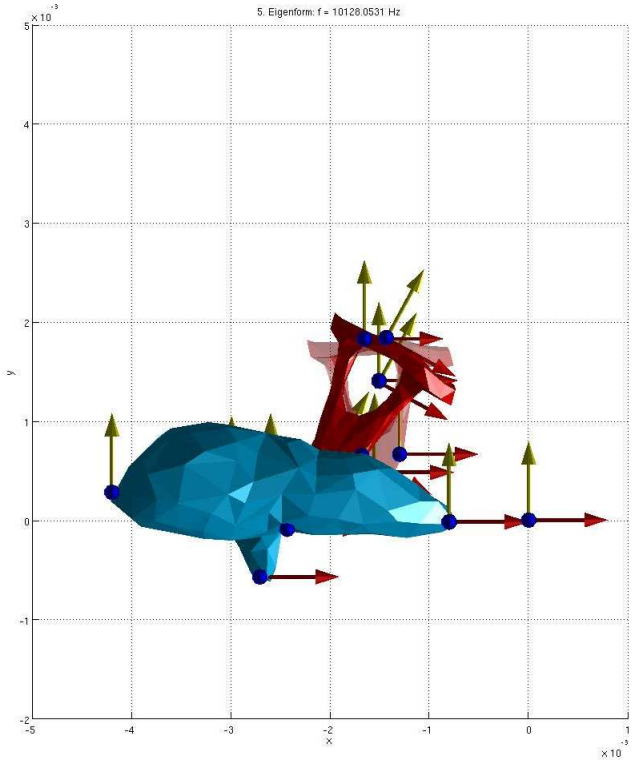

Figure 5.30: View of the fifth eigenmode.

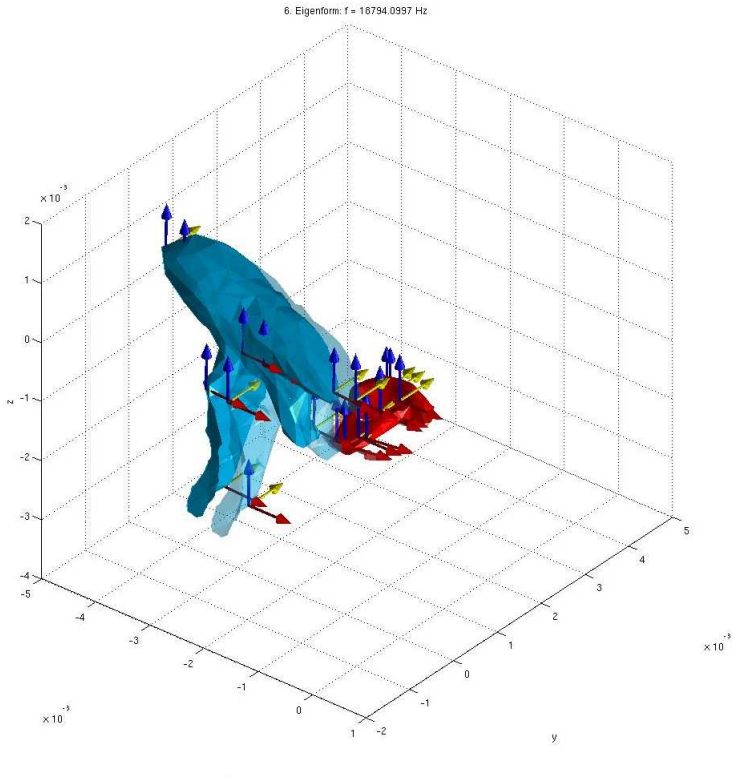

Figure 5.31: View of the sixth eigenmode.

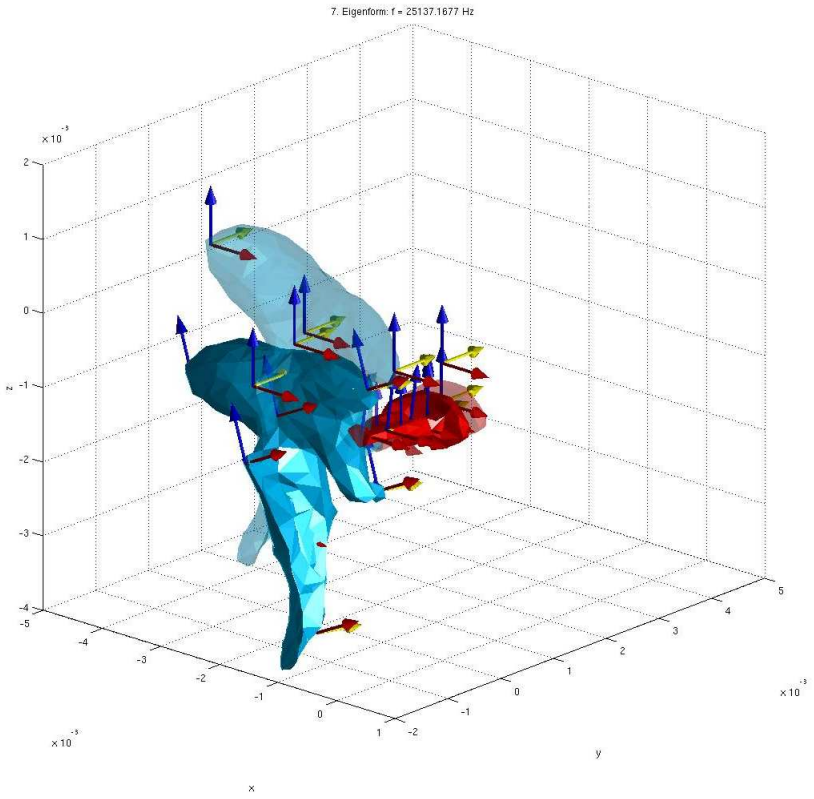

Figure 5.32: View of the seventh eigenmode.

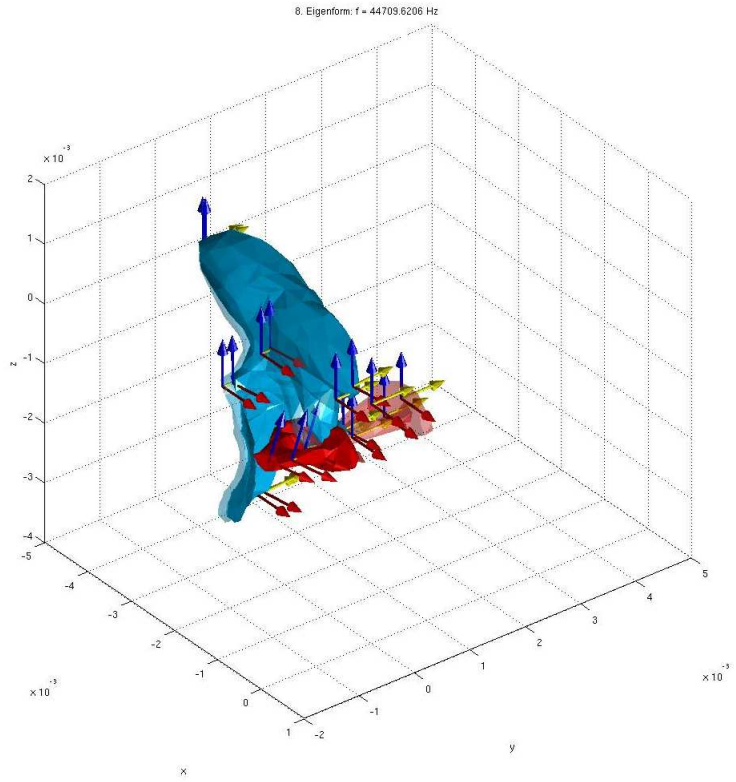

Figure 5.33: View of the eighth eigenmode.

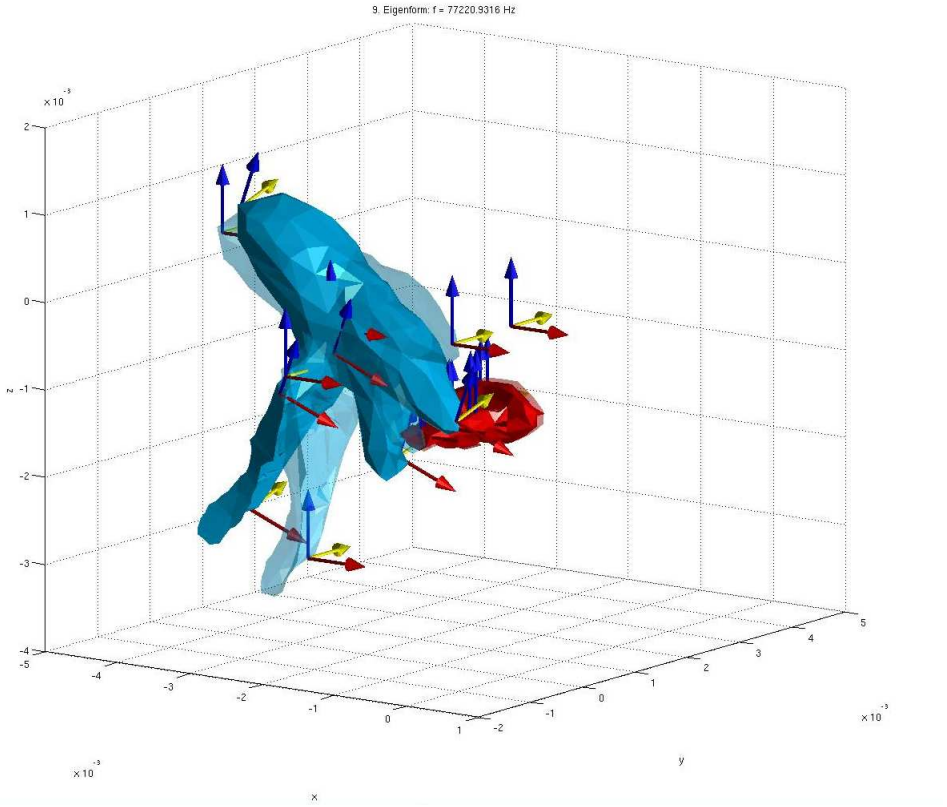

Figure 5.34: View of the ninth eigenmode.